Colloids and Surfaces A: Physicochem. Eng. Aspects 463 (2014) 37–43

Contents lists available at ScienceDirect

Colloids and Surfaces A: Physicochemical and Engineering Aspects

journal homepage: www.elsevier.com/locate/colsurfa

Release kinetics from LDH-drug hybrids: Effect of layers stacking and drug solubility and polarity

R. Rojas[a,*], A.F. Jimenez-Kairuz[b], R.H. Manzo[b], C.E. Giacomelli[a]

[a] INFIQC-CONICET, Departamento de Fisicoquímica, Facultad de Ciencias Químicas, Universidad Nacional de Córdoba, Ciudad Universitaria, 5000 Córdoba, Argentina

[b] UNITEFA-CONICET, Departamento de Farmacia, Facultad de Ciencias Químicas, Universidad Nacional de Córdoba, Ciudad Universitaria, 5000 Córdoba, Argentina

HIGHLIGHTS

- High drug loading, even exceeding anion exchange capacity, due to lateral interactions.
- Compact disposition of LDH-D hybrids when compressed, slowed surface reactions and diffusion.
- Faster release by anion exchange in neutral media, rate dependent on the apolar tail of the drug.
- Slow matrix weathering in acidic media, release rate and mechanism dependent on drug solubility.

GRAPHICAL ABSTRACT

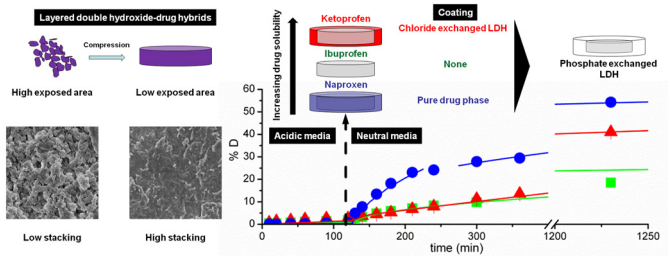

ARTICLE INFO

Article history:
Received 26 June 2014
Received in revised form
12 September 2014
Accepted 17 September 2014
Available online 28 September 2014

Keywords:
Zeta potential
Kinetics
Organic/inorganic hybrids
Hydrophobic interactions
Release mechanism

ABSTRACT

This work highlights the effect of drug solubility and polarity and solid layer stacking on the release rate and mechanism of layered double hydroxides-drug (LDH-D) hybrids. With such a purpose, LDH-D hybrids containing three structural related non-steroidal anti-inflammatory drugs (ibuprofen, naproxen or ketoprofen) were synthesized by a simple co-precipitation method. LDH matrixes exhibited a high drug loading capacity, even exceeding the anion exchange capacity of the solid especially with the more apolar drugs. The structure and interfacial properties of the particulate LDH-D hybrids were also dependent on the polarity of the loaded drug. Finally, the release mechanisms in neutral and acidic media were studied with compressed LDH-D hybrids. The hybrids compression leaded to highly stacked platelets that caused a slower and steadier drug release rate than particulate LDH-D hybrids in all cases. In neutral medium, the drugs were exclusively released by anion exchange with HPO_4^{2-} ions and the release rate was determined by the drug polarity. In acidic medium, weathering was the main release mechanism. However, additional processes (anion exchange, drug solubilization) were concurrent in the latter media, the overall mechanism and release rate being dependent on the drug solubility.

1. Introduction

Magnesium and aluminum layered double hydroxides (LDH) are biocompatible inorganic solids with brucite ($Mg(OH)_2$)-like structure. Isomorphic substitution of Mg^{2+} by Al^{3+} in the layers leads to a charge excess compensated by the introduction of anions in the interlayer space. They are able to incorporate organic anions, such as pharmaceutically active drugs [1,2], biomolecules [3–5], agrochemicals [6], plant growth regulators, food additives and dyes [7,8] by intercalation and/or adsorption, to prepare organic–inorganic hybrids. Anion release from these hybrids is produced by three mechanisms [9]: ion exchange (highly

* Corresponding author. Tel.: +54 351 4334169; fax: +54 351 4334188.
E-mail addresses: rrojas@fcq.unc.edu.ar, ricardorojasyd@gmail.com (R. Rojas).

http://dx.doi.org/10.1016/j.colsurfa.2014.09.031
0927-7757/

dependent on the anion nature and concentration of the release media), desorption and weathering (both processes depend on the pH of the release media).

Among the organic–inorganic hybrids, special attention has been paid to those including pharmaceutically active drugs (LDH-D); the main alleged advantages of LDH-D hybrids being drug preservation, release rate modification and, in some cases, bioavailability increment [10–12]. Particulate LDH-D hybrids prepared with non-steroidal anti-inflammatory drugs (NSAIDs), such as ibuprofen, naproxen or ketoprofen [13], show a slower release rate compared to the pure drug in intestinal media and an increased solubility of the acidic form of the drug in gastric media [9,14,15]. A great disadvantage of particulate LDH-D is the fast and complete release produced from the hybrids. However, the release rate from LDH-D can be reduced by increasing either the layers stacking or the particle size of the matrix. Guwanan and Xu [16] showed that the release rate of ibuprofen from LDH hybrids was determined by the aggregation of the LDH platelets. Similarly, Zhang et al. [17] showed that bigger particles leaded to longer release times from methotrexate-loaded LDHs. Surprisingly, there have been only a few comparative studies analyzing the incidence of the physicochemical properties of the drugs and the morphology of the solid on the release behavior from LDH-D hybrids [8].

In this work, the release rate from LDH-D hybrids was reduced by compressing the particulate solids into discs, which allowed studying the drugs release mechanisms and the effect of the drug physicochemical properties on the kinetic profiles in different media. Ibuprofen (Ibu), naproxen (Nap) or ketoprofen (Ket) were selected as interlayer anions, as they are structurally related NSAIDs. Biocompatible LDHs of Mg and Al, loaded with Ibu, Nap or Ket, were synthesized and characterized to determine the structure and interfacial properties of the hybrids. Particulate LDH-D was then compressed to obtain discs of densely packed hybrid particles. One- and two-steps kinetic experiments with compressed LDH-D hybrids were performed in acidic (0.05 mol L^{-1} phosphate buffer pH = 6.8) and/or in neutral (HCl pH = 1.2 + 0.05 mol L^{-1} NaCl) media and modeled to determine the drugs release mechanisms.

2. Materials and methods

Pharmaceutical grade Ibu, Ket and Nap (Parapharm®, Buenos Aires, Argentina) and reagent grade chemicals were used without further purification. Deionized water with a resistance of 18.2 MΩ was obtained using a Millipore ultrapurification system. The experiments were carried out at room temperature (25 °C) unless otherwise stated.

2.1. Synthesis

LDH-D hybrids (containing either Ibu, Nap or Ket) were synthesized by the coprecipitation method at constant pH [9,18]. A 0.1 L solution containing the metal ions (0.4 mol L^{-1} $AlCl_3$; 0.8 mol L^{-1} $MgCl_2$) was added drop wise to a 0.1 L solution containing 0.08 mol of the corresponding drug under vigorous stirring at pH = 9, controlled by addition of a 2 mol L^{-1} NaOH solution. The obtained slurries were centrifuged, washed and finally dried at 50 °C until constant weight. The hybrids were named LDH-Ibu, LDH-Ket and LDH-Nap according to the intercalated drug.

2.2. Structural and morphological characterization

Mg and Al content were determined by atomic absorption spectrometry in a Varian AA240 instrument. The samples were dissolved in HNO_3 and afterwards diluted to meet the calibration range. Dispersions of the hybrids in neutral medium (0.1 g L^{-1}, 0.05 M buffer phosphate, pH = 6.8) were prepared to determine their drug content using UV–vis spectrophotometry (Shimadzu UV1601, Japan). Water content was estimated by thermogravimetric analysis between 25 and 200 °C, carried out in a SETARAM Setsys Evolution 16/18 instrument at a 5 °C min^{-1} heating rate.

Powder X-ray diffraction (PXRD) patterns were recorded in a Phillips X'pert Pro instrument using a CuKα lamp (λ = 1.5408 Å) at 40 kV and 40 mA between 3° and 60° (2θ) in step mode (0.05°, 1.2 s). FT-IR spectra were measured in a FT-IR Bruker IFS28 instrument using KBr pellets (1:100 sample:KBr ratio). Scanning electron microscopy (SEM) images were obtained in a FE-SEM Σigma instrument on samples covered with a Cr layer.

The hydrodynamic apparent diameter (d) and zeta potential (ζ) of the samples were determined by dynamic light scattering (DLS) and electrophoretic light scattering (ELS) measurements, respectively, using a Delsa Nano C instrument (Beckman Coulter). Aqueous dispersions of the hybrids (0.1 g L^{-1} in $5{\cdot}10^{-2}$ mol L^{-1} NaCl) were prepared and sonicated for 30 min. Their d and ζ values were determined at different pH values, adjusted by addition of a NaOH solution. d and polydispersity values were calculated from the autocorrelation function ($g^{(2)}$) using the cumulants method, while electrophoretic mobilities were converted to ζ using the Smoluchowski equation. Contact angle (θ) measurements were performed by the sessile drop method using a homemade goniometer and deionized water drops over compressed LDH-D hybrids prepared at 2 tons with a 11 mm die. The experiments were performed in triplicate.

2.3. Drug release kinetics

Compressed LDH-D hybrids were prepared by compression of the corresponding sample (400 mg) in an 11 mm die at 2 tons. Two different degassed and thermostatized (37.0 ± 0.5 °C) release media were selected: acidic (HCl pH = 1.2 ± 0.1 in 0.05 mol L^{-1} NaCl) and neutral (0.05 mol L^{-1} phosphate buffer pH = 6.8 ± 0.1). SEM images of the compressed LDH-D hybrids before the different release experiments were also taken.

Drug release from compressed LDH-D hybrids in each release medium (one-step experiments) was studied in a dissolution test station (AT-7 smart, Sotax, Switzerland), using USP-method 2 (paddle, US Pharmacopeia, 2009 [19]) at 100 ± 1 rpm with 900 mL of dissolution media at 37.0 ± 0.5 °C. 4 mL of the samples were taken and filtered at defined time intervals up to 24 h, and replaced with an equivalent volume of fresh medium. The drug concentration was measured by UV–vis spectrophotometry at the corresponding absorbance maximum (λ = 264 nm, 271 nm and 260 nm for Ibu, Nap and Ket, respectively). Finally, a two-step release study was performed according to USP-method B (delayed-release dosage form, US Pharmacopeia, 2009 [19]). Namely, compressed LDH-D hybrids were tested for 2 h in acidic medium and then removed, rinsed with water and introduced in neutral medium, up to 24 h. All the experiments were conducted in triplicate to calculate the mean values and standard deviations included in the release profiles.

Separately, PXRD patterns, FTIR spectra and SEM images of the hybrids after the release experiments in acidic medium were also obtained. Compressed LDH-D hybrids were previously milled until a homogeneous powder was obtained.

Higuchi, zero order and Peppas kinetic models [20] were employed to fit the drug release behavior of the compressed LDH-D hybrids. However, Peppas model is the most general one and includes the other two models. The equation that describes Peppas model is:

$$\%D = \frac{M_t}{M_0} \cdot 100 = k_P t^n; \quad \log \%D = \log k_P + n \log t \tag{1}$$

where M_t is the amount of drug released at time t, M_0 is the initial drug content of LDH-D hybrid and k_P is the kinetic release constant.

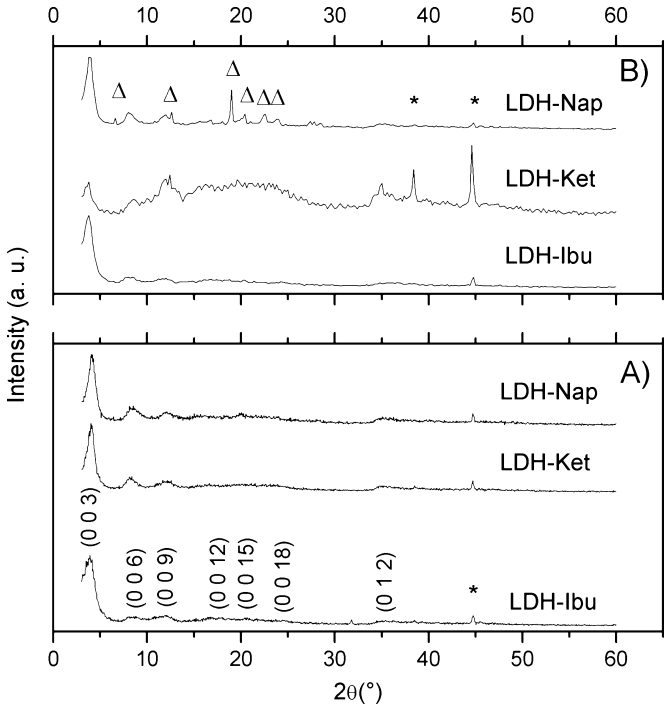

Fig. 1. PXRD patterns of the LDH-D hybrids as prepared (A), after 24 h contact with acidic media (B). Peaks of pure naproxen (Δ) and the aluminum holder (*) are also indicated.

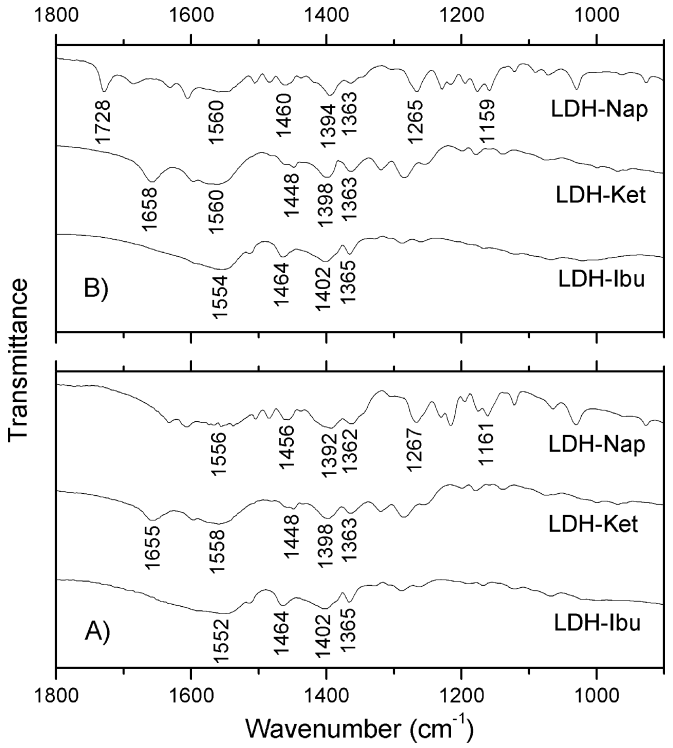

Fig. 2. FT-IR spectra of the LDH-D hybrids as prepared (A), after 24 h contact with acidic media.

Peppas model also includes a coefficient (n) that characterize the release mechanism: when $n = 1$, Peppas equation gives the same one as the zero order model, while $n = 0.5$ provides the Higuchi model. Although the system geometry affects these coefficients [21], for the purpose of this work n values close to 0.5 were associated with diffusion, as the rate determining step of the process, and values around 1 to surface reaction controlled kinetics. n and k_P values were calculated from the slopes and intercepts, respectively, of the linear fit [20] of *log %D* vs. *log t* plots (Supplementary material, Fig. S1).

3. Results and discussion

3.1. Structural and morphological characterization

PXRD patterns and FT-IR spectra were used to characterize the structure of the hybrids and to confirm the presence of the selected drug. The PXRD patterns (Fig. 1A) portrayed typical LDH features, such as narrow and symmetric peaks at 2θ below 30° and broad and asymmetric ones above this value [22]. These peaks were indexed in a rhombohedral lattice, the basal spacing values (Table 1) were in good accord with those reported by other authors for LDH-D hybrids, with Ibu [1,23], Nap [24,25] and Ket [14,26]. The (0 0 l) peaks presented high intensity compared to (0 1 2) ones (high (0 0 l)/(0 1 2) intensity ratio) in all cases, which pointed to a high ordering in the c axis direction. This feature of the PXRD patterns was considered indicative of exclusive intercalation with the corresponding drug [22].

On the other hand, the FT-IR spectra (Fig. 2A) of the hybrids showed bands related to the intercalated drug (between 1800 and 900 cm^{-1}), while bands of the hydroxide layers were registered at 900–400 cm^{-1} (not shown). All LDH-D hybrids presented bands corresponding to $\nu_{asym}(COO^-)$ and $\nu_{sym}(COO^-)$ at 1552–1558 cm^{-1} and 1392–1402 cm^{-1}, respectively, as well as bands at 1448–1464 cm^{-1} and 1362–1365 cm^{-1} due to $\delta(CH_2)$ [9]. The spectra also portrayed specific bands of each drug: a band at 1655 cm^{-1} assigned to the ketone group was observed in the case of LDH-Ket [14], while ν(C—O) and ν(C—O—C) bands of the ether group were registered for LDH-Nap at 1267 and 1161 cm^{-1}, respectively [27]. None of the hybrids displayed bands at 1700–1750 cm^{-1} corresponding to ν(COOH), which indicated the absence of the drug acid form [28].

In good accord with the structural characterization, the chemical composition and formulae of the hybrids (Table 1) established that the drug content was, at least, equal to the calculated anion exchange capacity, deduced from the Al^{3+} content of the layers [29]. Furthermore, both LDH-Ibu and LDH-Nap presented a drug excess (20 and 1%, respectively) similar to those previously obtained for other anions, such as Ibu itself or dodecylsulfate [9,29]. This excess indicated that these drugs were incorporated not only by electrostatic interactions with the positively charged layers, but also by specific adsorption, due to lateral interactions between their hydrophobic tails [30]. Accordingly, the excess followed the sequence Ibu > Nap > Ket, parallel to the *log P* values (Supplementary material, Table S1), related to the presence of polar groups,

Table 1
Chemical composition and formula, cell parameters and contact angle (*CA*) measurements of the LDH-D hybrids.

Sample	%Mg	%Al	% drug	Chemical formula	a (Å)	c (Å)	θ (°)[a]
LDH-Ibu	11.0	5.2	53.4	$Mg_{2.4}Al(OH)_{6.8}Ibu_{1.20}\cdot 2.4\ H_2O$	3.04	66.3	86 ± 4
LDH-Nap	11.9	5.3	47.8	$Mg_{2.5}Al(OH)_7Nap_{1.01}\cdot 4.1\ H_2O$	3.02	66.6	72 ± 4
LDH-Ket	10.5	4.9	44.2	$Mg_{2.4}Al(OH)_{6.8}Ket_{0.95}\cdot 5.9\ H_2O$	3.03	66.0	65 ± 3

[a] Contact angle.

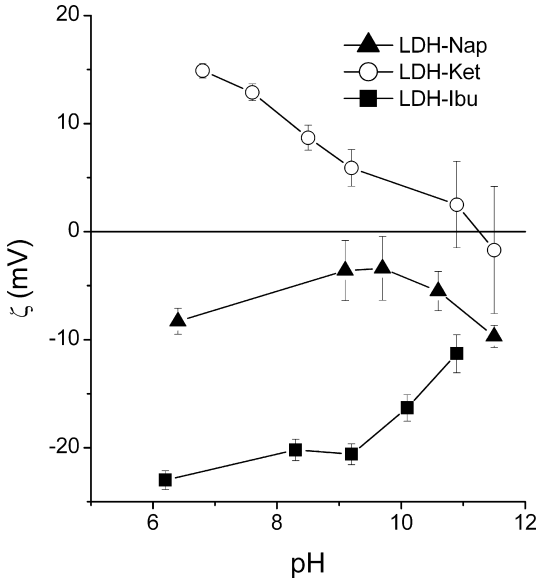

Fig. 3. ζ vs. pH curves of LDH-Ibu (squares), LDH-Ket (circles) and LDH-Nap hybrids (triangles) hybrids.

such as ether and ketone in the case of Ket and Nap, respectively (Supplementary material, Fig. S2).

In line with its anion excess, LDH-Ibu hybrid presented negative ζ values in the measured pH range (Fig. 3), a behavior similar to that observed for anions with chemical affinity for LDHs [9,29]. On the other hand, LDH-Ket hybrid showed positively charged particles at pH = 7 and ζ decreased with increasing pH, a behavior similar to that of LDH intercalated with anions exclusively bond by electrostatic interactions [29]. Finally, LDH-Nap hybrid presented an intermediate behavior, in agreement with the lower anion excess compared to LDH-Ibu. The contact angle (θ) values of the compressed LDH-D hybrids (Table 1, Supplementary material, Fig. S3A, C and E) were also concordant with this sequence, as LDH-Ibu hybrid presented the most hydrophobic surface, followed by LDH-Nap and LDH-Ket. Moreover, this sequence also affected the wettability of the compressed hybrids (Supplementary material, Fig. S3B, D and F). It was low for LDH-Ibu and LDH-Nap, the water drops being stable during the θ determination, while it was high for LDH-Ket, the drops wetting the discs after a few seconds.

The particle size and shape of particulate LDH-D hybrids were assessed by DLS determinations and SEM images. Fig. 4 shows the images of LDH-Ibu, which are representative of the general behavior; the images of the other hybrids being included as Supplementary material, Fig. S4. According to DLS measurements, LDH-D hybrids presented large *d* (around 6–10 μm) and high polydispersity in all cases (data not shown). On the other hand, the SEM images showed that these particles were formed by agglomeration of smaller units or platelets of around 300 nm (Fig. 4A). These platelets presented high diameter to thickness ratio, irregular shape and a loose disposition [31]. The compression of particulate LDH-D hybrids produced densely packed discs where the platelets arrangement became dense and compact, but their aspect was similar to that before compression (Fig. 4B).

3.2. Drug release kinetics

Drug release profiles from compressed LDH-D hybrids were followed in either one-step (acidic or neutral medium) or two-steps (acidic followed by neutral medium) experiments (Fig. 5). In general, the drug release from the compressed LDH-D hybrids was slower than that previously measured for the particulate solid

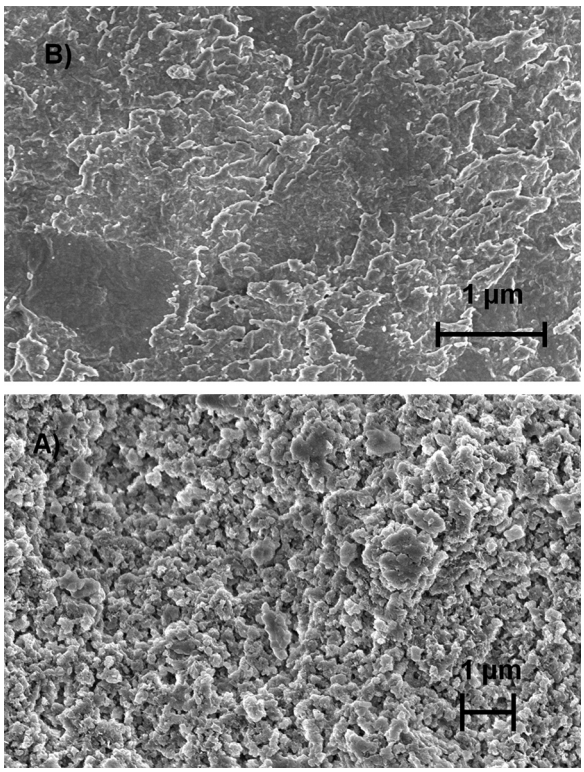

Fig. 4. SEM images of LDH-Ibu hybrids as particulate solid (A) and compressed into discs (B).

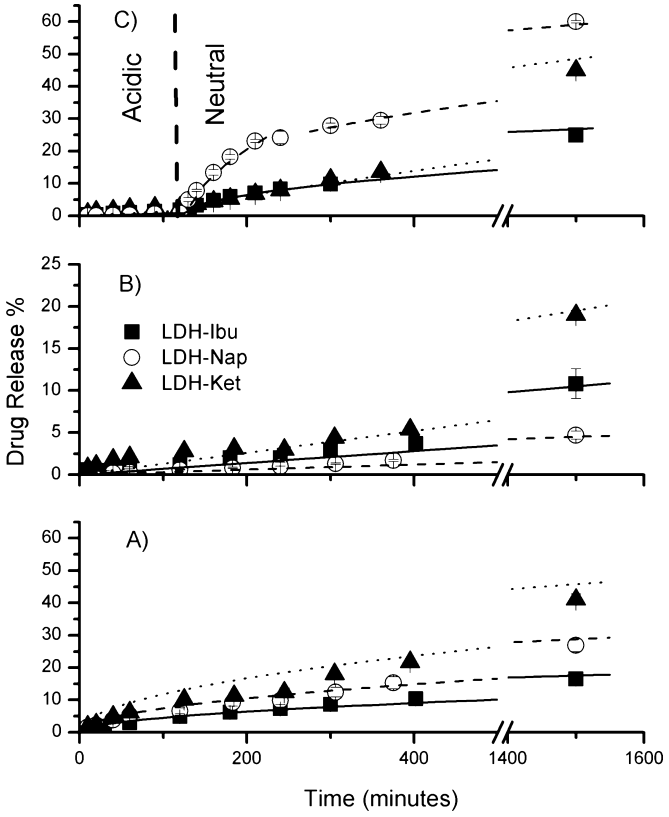

Fig. 5. Drug release kinetics of the compressed LDH-D hybrids performed in one-step in neutral (A) or acidic (B) media, and in two-step (acidic followed by neutral medium) experiments. Experimental data (symbols) and fitted profiles (lines).

Table 2
Kinetic data for drug release from LDH hybrids compacted as discs.

Sample	Medium	Zero order		Peppas			Higuchi	
		k_Z[a]	R^2	n	k_P[b]	R^2	k_H[c]	R^2
LDH-Ibu	Acid	0.013	0.642	0.6	0.269	0.988	0.449	0.984
	Neutral	0.008	0.983	0.8	0.033	0.997	0.233	0.892
LDH-Nap	Acid	0.022	0.621	0.6	0.434	0.993	0.702	0.987
	Neutral	0.003	0.976	0.9	0.007	0.997	0.097	0.855
LDH-Ket	Acid	0.035	[a]0.788	0.6	0.522	0.990	1.029	0.963
	Neutral	0.014	0.968	0.6	0.164	0.998	0.379	0.799

[a] in %/min.
[b] in %/min^n.
[c] in %/min$^{0.5}$.

[9,14,24]. This behavior was due to the compact disposition of LDH-D platelets, leading to longer diffusion paths [16]. Another important variation to that observed for the particulate solid was the absence of burst release at the beginning of the experiments. This effect was a direct result of the compacted arrangement of the platelets that diminished the exposed surface area.

A steady, slow release from LDH-D hybrids was obtained in neutral medium (Fig. 5A). After 24 h, only 16.5, 27.0, and 41.0% of the drug loading was released from LDH-Ibu, LDH-Nap and LDH-Ket, respectively. The release rate followed the sequence Ket > Nap > Ibu, which was consistent with the increasing lateral interactions and specific adsorption in the order Ket < Nap< Ibu. Peppas kinetic model (Eq. (1)) was used for the interpretation of the drug release mechanism from the compressed LDH-D hybrids, the obtained kinetic constant values are included in Table 2. In neutral medium, fitting the experimental profiles produced n values close to 0.5 indicating diffusion controlled kinetics in all cases. Therefore, similarly to that observed in particulate solid formulation, drug release was produced by anion exchange, a diffusion controlled process, that can be described by the following equilibrium [9]:

$$\text{LDH-D}_{(s)} + \text{HPO}_4{}^{2-}{}_{(aq)} \leftrightarrow \text{LDH-HPO}_{4(s)} + 2\text{D}^-{}_{(aq)} \quad (2)$$

where $HPO_4{}^{2-}$ was the only exchanging anion due to the higher affinity of divalent anions for LDH [9]. k_P values were consistent with the experimental observed sequence, the solid being increasingly exchanged with $HPO_4{}^{2-}$ ions in the order Ket > Nap > Ibu. The release rate was then determined mainly by the polarity of the drug, which also affected the hydrophobicity and wettability of the discs and, consequently, the diffusion capacity of phosphate anions. In comparison to that obtained for the particulate solid, drug release in neutral medium was slower due to the longer diffusion paths while the exposed area diminution leaded to the inhibition of surface processes such as desorption, preventing the burst effects observed in previous studies.

Similarly to that observed in neutral medium, release from LDH-D hybrids was slow and steady in acidic medium (Fig. 5B). The release profiles in acidic medium indicated that less than 20% of the drug was released after 24 h in all cases. The release rate followed the sequence Ket > Ibu > Nap, parallel to the decreasing drug solubility (Supplementary material, Table S1). Contrarily to that observed for non-compressed solids [9,14], the drug solubility in acidic medium was not reached within the measured time range. The concentration of the corresponding drug, dissolved in the release acidic medium, at t = 24 h was 51%, 21% and 31% of the drug solubility for LDH-Ibu, LDH-Ket and LDH Nap, respectively. This result indicated that the LDH matrix was not completely dissolved during the experiments.

According to the literature, weathering is the only release mechanism in acidic medium with particulate LDH-D hybrids. LDH layers are rapidly and completely dissolved in acidic media and the drug is fully released within a few minutes [9]. Nevertheless, only a fraction of the released drug is dissolved due to its low solubility in acidic medium. Both processes were slower in compressed LDH-D hybrids due to the reduced exposed surface area of the platelets and, consequently, the LDH layers were only partially dissolved and the drug solubility was not reached in the time range of the experiments. In any case, drug release by weathering is a surface reaction controlled process that can be described by the following equilibria [9]:

$$\text{LDH-D}_{(s)} + \text{H}^+{}_{(aq)} \leftrightarrow \text{HD}_{(s)} + \text{Mg}^{2+}{}_{(aq)} + \text{Al}^{3+}{}_{(aq)} + \text{H}_2\text{O} \quad (3)$$

$$\text{HD}_{(s)} \leftrightarrow \text{HD}_{(aq)} \quad (4)$$

As weathering is a surface reaction controlled process, n values near 1 for Peppas model were expected. Surprisingly, although n was near 1 for LDH-Nap, this parameter decreased in the order Nap > Ibu > Ket (Table 2), indicating that diffusion increasingly controlled the release rate in this sequence. In good accord the ln % vs. t curves (Supplementary material, Fig. S1) were not parallel, contrarily to that obtained in neutral media.

In order to study this mechanism change when loading different NSAIDs to LDH matrixes, the discs were milled after the experiments and the resulting powder was studied by PXRD (Fig. 1B) and FT-IR (Fig. 2B). PXRD patterns of LDH-Nap showed peaks of a pure Nap phase, which was confirmed by the band at 1728 cm^{-1} (Fig. 2C) ascribed to the carbonyl vibration mode of COOH group [28]. Neither pure drug phases nor COOH group bands were registered for LDH-Ibu or LDH-Ket, which discarded the presence of the acid form of the drug. Nevertheless, the decreasing (0 0 l)/(0 1 2) intensity ratio observed in the PXRD of LDH-Ket indicated that this hybrid was not exclusively intercalated with the drug after 24 h in contact with acidic medium. The different behavior of the hybrids was also reflected on the surface of the discs, as shown by the SEM images (Fig. 6A–C). LDH-Ket hybrid (Fig. 6C) showed a loose arrangement of the platelets and LDH-Nap (Fig. 6B) exhibited a coating of small particles, consistent with the presence of a pure drug phase. On the contrary, compressed LDH-Ibu hybrid presented similar surface topography before (Fig. 4B) and after (Fig. 6A) the release experiment.

From these results it was deduced that Nap dissolution (Eq. [4]) was slower than LDH-Nap erosion (Eq. [3]) due to the low solubility of the drug (Supplementary material, Table S1), being drug dissolution the surface process that controlled the release kinetics. The slow Nap dissolution was responsible for the presence of the pure Nap phase determined by both PXRD patterns and FT-IR spectra and the Nap coating on the LDH-Nap disk surface observed on the SEM images. On the contrary, the dissolution of Ket was faster than LDH-Ket weathering and additional drug was supplied by anion exchange with chloride:

$$\text{LDH-Ket}_{(s)} + \text{H}^+{}_{(aq)} + \text{Cl}^-{}_{(aq)} \leftrightarrow \text{LDH-Cl}_{(s)} + \text{HKet}_{(s)} \quad (5)$$

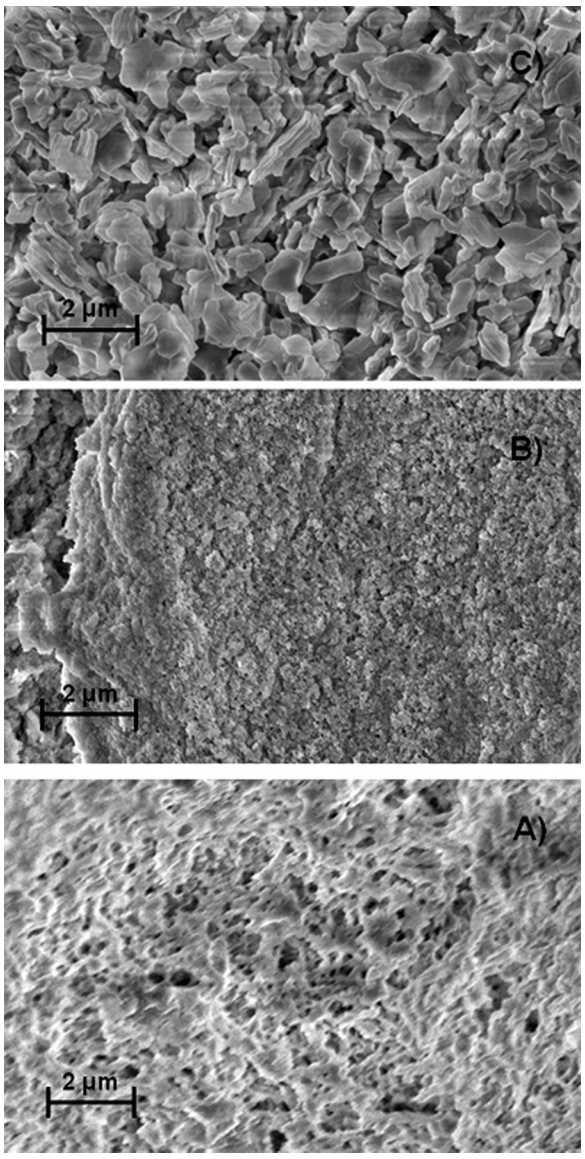

Fig. 6. SEM microphotographs of discs containing LDH-Ibu (A), LDH-Nap (B), and LDH-Ket (C) after dissolution tests in acidic medium.

This process leaded to partially Cl^- exchanged LDH particles intercalated with Ket, produced the intensity decrease of the (0 0 *l*) peaks observed XRD patterns (Fig. 1B) while the SEM images of LDH-Ket tablet demonstrated the presence of LDH-like particles with a loose disposition. Finally, in the case of Ibu, the rates of LDH weathering and drug release were similar, the composition and morphology of disk surface at the end of the experiment being quite similar to that at the beginning.

In order to confirm the presence and composition of the coating produced in acidic medium, two-steps experiments were performed. Compressed LDH-D hybrids were first immersed in acidic medium for 2 h, rinsed with water and introduced in neutral medium up to 24 h. Fig. 5C shows the release profiles of the consecutive two-steps (acidic + neutral media) release experiments. As expected, the main drug release was produced during the second step in all cases. In the case of LDH-Nap and LDH-Ket, the drug release behavior during the second step was significantly different to that obtained for the single-step experiments in neutral medium. Nap release profile showed a fast release (20% in 60 min) at the beginning of the second step, followed by a sustained release until 24 h. Contrarily, LDH-Ket showed a slight release rate decrease during the first minutes of the second step compared to that observed in the one-step experiment in neutral medium. Finally, LDH-Ibu release remained almost unaffected with respect to that in the one-step experiment.

The behavior of compressed LDH-D hybrids in the two-step experiments was related to the release mechanism in acidic media and the composition of the solid in the external layer of the discs. Thus, the burst effect for LDH-Nap was due to the presence of the pure drug coating, which was dissolved in neutral media. The effect was the opposite for LDH-Ket, as the phosphate anions found a barrier of partially exchanged LDH. Finally, as LDH-Ibu disk presented no external coating after the first step, its behavior was identical to that obtained for the single-step neutral media experiment.

4. Conclusions

LDH-D hybrids containing NSAIDs (ibuprofen, naproxen or ketoprofen) were synthesized by a simple method that produced large loading capacities, even exceeding the anion exchange capacity of the matrix. These particulate hybrids were easily compacted, which led to hard discs with a condensed disposition of platelets. As a consequence, diffusion and surface controlled reactions were hindered by the long diffusion paths and the low exposed surface area, respectively. Drug release was slower than that obtained for the particulate solid in all cases, indicating the importance of particle stacking in the release behavior of LDH-D hybrids. In neutral media (0.05 mol L^{-1} phosphate buffer pH = 6.8), the release mechanism was exclusively anion exchange between the drugs and HPO_4^{2-} ions. In this medium, the release rate was determined by the affinity of the drug for the LDH layers, controlled by the polarity of the drug tail. On the other hand, the main release mechanism in acidic medium (HCl pH = 1.2 + 0.05 mol L^{-1} NaCl) was the solid weathering, a slow process that was not complete within 24 h. Both the release rate and the rate determining step were determined by the drug solubility in acidic media. Thus, Nap dissolution was slower than the hybrids dissolution, leading to the formation of a coating of pure drug. On the other hand, all released Ibu and Ket from the compressed hybrids was dissolved. Moreover, due to the high solubility of Ket, anion exchange reactions were also concurrent. The results here provided present potential applications in the design of vehicles of organic anions, such as drugs, agrochemicals, food additives with a fine tuning of their release profiles.

Acknowledgements

Economic support by SeCyT-UNC project number 05/C585, FONCyT, project numbers 12/0634 and 10/2116, and CONICET, PIP 11220120100575, are gratefully acknowledged. We thank the technical support of LARMARX-FAMAF-UNC to obtain the SEM images.

Appendix A. Supplementary data

Supplementary data associated with this article can be found, in the online version, at http://dx.doi.org/10.1016/j.colsurfa.2014.09.031.

References

[1] U. Costantino, V. Ambrogi, M. Nocchetti, L. Perioli, Hydrotalcite-like compounds: versatile layered hosts of molecular anions with biological activity, Microporous Mesoporous Mater. 107 (2008) 149–160.
[2] J.H. Choy, J.M. Oh, S.J. Choi, Layered double hydroxides as controlled release materials, in: P. Ducheyne (Ed.), Comprehensive Biomaterials, Elsevier, Oxford, 2011, pp. 545–557.
[3] Y. Wong, K. Markham, Z.P. Xu, M. Chen, G.Q. Max Lu, P.F. Bartlett, et al., Efficient delivery of siRNA to cortical neurons using layered double hydroxide nanoparticles, Biomaterials 31 (2010) 8770–8779.

[4] J. Choy, S. Choi, J. Oh, T. Park, Clay minerals and layered double hydroxides for novel biological applications, Appl. Clay Sci. 36 (2007) 122–132.
[5] X. Kong, S. Shi, J. Han, F. Zhu, M. Wei, X. Duan, Preparation of Glycy-L-tyrosine intercalated layered double hydroxide film and its in vitro release behavior, Chem. Eng. J. 157 (2010) 598–604.
[6] Q. Zhenlan, Y. Heng, Z. Bin, H. Wanguo, Synthesis and release behavior of bactericides intercalated Mg–Al layered double hydroxides, Colloids Surf. A: Physicochem. Eng. Asp. 348 (2009) 164–169.
[7] J.-M. Oh, T.T. Biswick, J.-H. Choy, Layered nanomaterials for green materials, J. Mater. Chem. 19 (2009) 2553.
[8] A.I. Khan, A. Ragavan, B. Fong, C. Markland, M. O'Brien, T.G. Dunbar, et al., Recent developments in the use of layered double hydroxides as host materials for the storage and triggered release of functional anions, Ind. Eng. Chem. Rev. 48 (2009) 10196–10205.
[9] R. Rojas, M.C. Palena, A.F. Jimenez-Kairuz, R.H. Manzo, C.E. Giacomelli, Modeling drug release from a layered double hydroxide–ibuprofen complex, Appl. Clay Sci. 62–63 (2012) 15–20.
[10] M. Wei, M. Pu, J. Guo, J. Han, F. Li, J. He, et al., Intercalation of L-dopa into layered double hydroxides: enhancement of both chemical and stereochemical stabilities of a drug through host–guest interactions, Chem. Mater. 20 (2008) 5169–5180.
[11] V. Bugatti, G. Gorrasi, F. Montanari, M. Nocchetti, L. Tammaro, V. Vittoria, Modified layered double hydroxides in polycaprolactone as a tunable delivery system: in vitro release of antimicrobial benzoate derivatives, Appl. Clay Sci. 52 (2011) 34–40.
[12] L. Perioli, V. Ambrogi, L. di Nauta, M. Nocchetti, C. Rossi, Effects of hydrotalcite-like nanostructured compounds on biopharmaceutical properties and release of BCS class II drugs: the case of flurbiprofen, Appl. Clay Sci. 51 (2011) 407–413.
[13] V. Rives, M. Del Arco, C. Martín, Layered double hydroxides as drug carriers and for controlled release of non-steroidal antiinflammatory drugs (NSAIDs): a review, J. Control. Release 169 (2013) 28–39.
[14] V. Ambrogi, G. Fardella, G. Grandolini, M. Nocchetti, L. Perioli, Effect of hydrotalcite-like compounds on the aqueous solubility of some poorly water-soluble drugs, J. Pharm. Sci. 92 (2003) 1407–1418.
[15] M.L. Parello, R. Rojas, C.E. Giacomelli, Dissolution kinetics and mechanism of Mg–Al layered double hydroxides: a simple approach to describe drug release in acid media, J. Colloid Interface Sci. 351 (2010) 134–139.
[16] P. Gunawan, R. Xu, Direct control of drug release behavior from layered double hydroxides through particle interactions, J. Pharm. Sci. 97 (2008) 4367–4378.
[17] X.-Q. Zhang, M.-G. Zeng, S.-P. Li, X.-D. Li, Methotrexate intercalated layered double hydroxides with different particle sizes: structural study and controlled release properties, Colloids Surf. B: Biointerfaces 117C (2014) 98–106.
[18] X. Duan, J. Lu, D.G. Evans, Assembly chemistry of anion-intercalated layered materials, in: Q. Xu, R. Pang, W. Huo (Eds.), Modern Inorganic Synthetic Chemistry, Elsevier B.V., 2011, pp. 375–404.
[19] United States Pharmacopeia, The National Formulary USP32-NF27, 2009.
[20] P. Costa, J.M. Sousa Lobo, Modeling and comparison of dissolution profiles, Eur. J. Pharm. Sci. 13 (2001) 123–133.
[21] J. Siepmann, N.A. Peppas, Modeling of drug release from delivery systems based on hydroxypropyl methylcellulose (HPMC), Adv. Drug Deliv. Rev. 48 (2001) 139–157.
[22] D.G. Evans, R.T.C. Slade, Structural aspects of layered double hydroxides, in: X. Duan, D.G. Evans (Eds.), Layered Double Hydroxides, 2006, pp. 1–87.
[23] V. Ambrogi, G. Fardella, G. Grandolini, L. Perioli, Intercalation compounds of hydrotalcite-like anionic clays with antiinflammatory agents – I. Intercalation and in vitro release of ibuprofen, Int. J. Pharm. 220 (2001) 23–32.
[24] D. Carriazo, M. del Arco, C. Martín, C. Ramos, V. Rives, Influence of the inorganic matrix nature on the sustained release of naproxen, Microporous Mesoporous Mater. 130 (2010) 229–238.
[25] M. del Arco, A. Fernandez, C. Martin, V. Rives, Release studies of different NSAIDs encapsulated in Mg, Al, Fe-hydrotalcites, Appl. Clay Sci. 42 (2009) 538–544.
[26] M.S. San Román, M.J. Holgado, B. Salinas, V. Rives, Characterisation of diclofenac, ketoprofen or chloramphenicol succinate encapsulated in layered double hydroxides with the hydrotalcite-type structure, Appl. Clay Sci. 55 (2012) 158–163.
[27] M. del Arco, S. Gutiérrez, C. Martín, V. Rives, J. Rocha, Synthesis and characterization of layered double hydroxides (LDH) intercalated with non-steroidal anti-inflammatory drugs (NSAID), J. Solid State Chem. 177 (2004) 3954–3962.
[28] K. Nakamoto, Infrared and Raman Spectra of Inorganic and Coordination Compounds, 5th ed., Wiley and Sons, New York, 1997.
[29] R. Rojas, F. Bruna, C.P. de Pauli, M.Á. Ulibarri, C.E. Giacomelli, The effect of interlayer anion on the reactivity of Mg–Al layered double hydroxides: improving and extending the customization capacity of anionic clays, J. Colloid Interface Sci. 359 (2011) 136–141.
[30] R. Rojas, C.E. Giacomelli, Effect of structure and bonding on the interfacial properties and the reactivity of layered double hydroxides and Zn hydroxide salts, Colloids Surf. A: Physicochem. Eng. Asp. 419 (2013) 166–173.
[31] Y. Zhang, J.R.G. Evans, Alignment of layered double hydroxide platelets, Colloids Surf. A: Physicochem. Eng. Asp. 408 (2012) 71–78.